The EMBO Journal (2004) 23, 4330–4341 | © 2004 European Molecular Biology Organization | All Rights Reserved 0261-4189/04
www.embojournal.org

THE EMBO JOURNAL

Macrodomain organization of the *Escherichia coli* chromosome

Michèle Valens[1], Stéphanie Penaud[1], Michèle Rossignol[1], François Cornet[2] and Frédéric Boccard[1,*]

[1]Centre de Génétique Moléculaire du CNRS, Gif-sur-Yvette, France and [2]Laboratoire de Microbiologie et Génétique Moléculaire du CNRS, Toulouse, France

We have explored the *Escherichia coli* chromosome architecture by genetic dissection, using a site-specific recombination system that reveals the spatial proximity of distant DNA sites and records interactions. By analysing the percentages of recombination between pairs of sites scattered over the chromosome, we observed that DNA interactions were restricted to within subregions of the chromosome. The results indicated an organization into a ring composed of four macrodomains and two less-structured regions. Two of the macrodomains defined by recombination efficiency are similar to the Ter and Ori macrodomains observed by FISH. Two newly characterized macrodomains flank the Ter macrodomain and two less-structured regions flank the Ori macrodomain. Also the interactions between sister chromatids are rare, suggesting that chromosome segregation quickly follows replication. These results reveal structural features that may be important for chromosome dynamics during the cell cycle.
The EMBO Journal (2004) **23,** 4330–4341. doi:10.1038/sj.emboj.7600434; Published online 7 October 2004
Subject Categories: genome stability & dynamics
Keywords: bacterial chromosome; chromatids cohesion; chromosome conformation; macrodomain; site-specific recombination

Introduction

The large size of genomes compared to the cell dimensions imposes condensation of chromosomes but the understanding of chromosome architecture and spatial organization remains unclear. In eukaryotic cells, chromosomes are not distributed in a disorderly manner in the interphase nucleus; instead, each chromosome occupies a defined, mutually exclusive fraction of the nuclear space referred to as a chromosome territory (Parada and Misteli, 2002). Although models of nonrandom nuclear chromosome organization emerge, the nature of territories and the molecular bases that enhance or restrain chromosome movements during the cell cycle are poorly understood. The bacterial chromosome, named a nucleoid, is a compact structure containing independent supercoiling domains (for review, see Higgins, 1999; Sherratt, 2003). Supercoiling domains were recently shown to be smaller and more labile than previously believed (averaging roughly 10 kb) and barriers delimiting domains being created and destroyed in intervals considerably less than a generation time (Deng *et al*, 2004; Postow *et al*, 2004). The circular bacterial chromosome has been shown to be organized with a particular orientation inside the cell that preserves the linear order of genes on the DNA (Teleman *et al*, 1998; Wu and Errington, 1998; Niki *et al*, 2000; Viollier *et al*, 2004). Bacteria replicate their chromosomes at a central replisome relatively stationary through which the DNA template passes as it is replicated (Lemon and Grossman, 2000; Espéli *et al*, 2003). Replication initiates from a single origin, *oriC*, and progresses bidirectionally. Soon after duplication, the two origins move from a midcell location to positions in the two halves of the cell, whereas the terminus is found at midcell and quarter points in between (Teleman *et al*, 1998; Niki *et al*, 2000). In *Escherichia coli*, a *cis*-acting 25-bp palindromic site, *migS*, plays a crucial role in bipolar positioning of *oriC* (Yamaichi and Niki, 2004). Because chromosome segregation and chromosome folding occur concurrently in bacteria, regions of the chromosome appear to be partitioned soon after their replication even as the remainder of the chromosome awaits replication. Analysis of how the SMC-like protein MukBEF condensates DNA revealed its likely involvement in organizing the chromosome in a series of loops orthogonal to the cell axis (Case *et al*, 2004), which might account for the orderly arrangement of the chromosome (Breier and Cozzarelli, 2004). In *Bacillus subtilis* and *E. coli*, several phenomena have been reported that suggest a spatial organization of the chromosome in the cell. For example, in *B. subtilis*, specific regions have been shown to be required for chromosome positioning in sporulating cells (Wu and Errington, 2002; Ben-Yehuda *et al*, 2003). In addition, the Par-like protein SpoOJ contributes to the *ori* region organization by binding numerous *parS* sites scattered over 800 kb (Lee *et al*, 2003 and references therein). In *E. coli*, FISH analyses have revealed the existence of two macrodomains, the Ori and Ter macrodomains, defined as large regions of about 1 megabase (Mb) that localize precisely in the cell (Niki *et al*, 2000). Macrodomains are not static and they have been observed to relocate at specific positions during the cell cycle (Niki *et al*, 2000). The exact nature of macrodomains and the role they play in cell cycle-dependent localization of the chromosome remain to be defined.

Three different genetic systems have been used to probe *in vivo* the structure of *E. coli* or *Salmonella* nucleoid: the γδ Res system (Higgins *et al*, 1996; Higgins, 1999), the transposon Tn*7* immunity system (DeBoy and Craig, 1996) and the λ Int system (Garcia-Russell *et al*, 2004). The first two systems did not reveal genome-wide DNA interactions, and frequency of interactions was decreasing proportionally with the increase in the distance between the sites. This feature might

*Corresponding author. Centre de Génétique Moléculaire du CNRS, Avenue de la Terrasse, 91198 Gif-sur-Yvette, France.
Tel.: +33 1 6982 3211; Fax: +33 1 6982 3150;
E-mail: boccard@cgm.cnrs-gif.fr

Received: 30 July 2004; accepted: 9 September 2004; published online: 7 October 2004

result from the intrinsic properties of the systems used: in γδ Res, synapsis of recombining sites results obligatory from plectonemic DNA slithering with the trap of three negative supercoils and this feature imposes one-dimensional interactions. Based on 20 intervals, probing the *Salmonella* chromosome structure with the λ site-specific recombination system has revealed that the *Salmonella* chromosome is not completely fluid but rather organized in some way.

To further describe chromosome organization in *E. coli* and characterize parameters that may control its folding and DNA dynamics, we have developed a genetic system that reports the relative probabilities that different pairs of loci scattered over the genome collide with one another. The existence of macrodomains or of other organized regions should bias the relative probabilities of collision between distant DNA sites in the chromosome. The site-specific recombination system of bacteriophage λ has been extensively characterized (for review, see Azaro and Landy, 2002) and recombination between λ *att* sites is appropriate to disclose the conformation of the bacterial chromosome. We have constructed several series of strains containing one defined *att* site at a fixed position and its *att* partner site inserted at various locations. We subsequently selected strains that were able to support recombination between *att* sites. The percentages of recombination observed with sites scattered over the chromosome were recorded and reported as a function of the location on the chromosome map. These results reveal a strong bias in the selection of DNA sites, in support of a highly ordered organization of the bacterial chromosome consisting of four macrodomain-like regions and two less-constrained regions.

Results

Probing chromosome organization by measuring long-range DNA interactions

The analysis of long-range DNA interactions relies on the availability of a system that can record these communications. DNA transactions promoted by λ Int (Azaro and Landy, 2002) are appropriate to reveal DNA collisions in the cell for the following reasons: (i) synapsis of *att* sites occurs by random collision, therefore the frequency of recombination between *att* sites will indicate their spatial proximity (Crisona *et al*, 1999); (ii) Int is a versatile recombinase that can recombine sites in direct or inverse orientation, located on the same molecule or on separate molecules (Figure 1); and (iii) Int mediates phage integration in the chromosome by recombination between phage *att*P and bacterial *att*B attachment sites (integrative recombination) generating two hybrid sites, *att*L and *att*R. Recombination between *att*L and *att*R (excisive recombination) requires the additional presence of

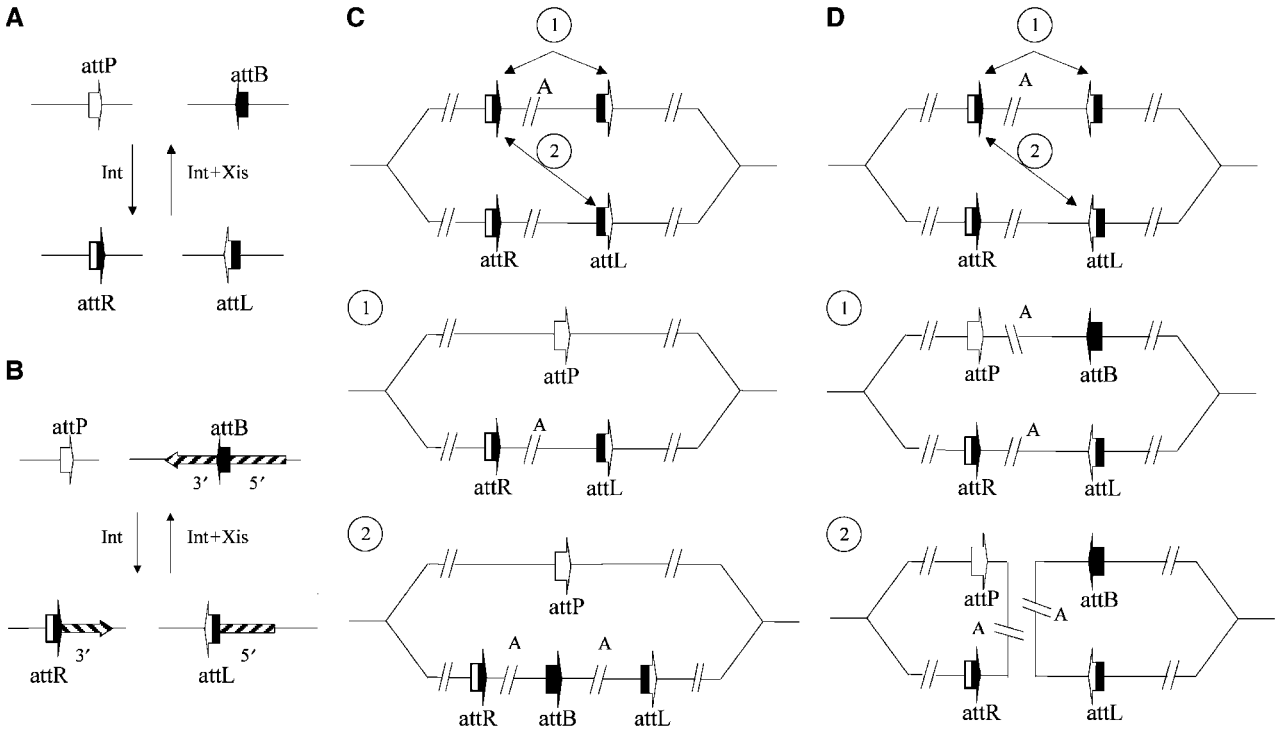

Figure 1 Versatility of the site-specific recombination system of phage lambda and recombination scenarios between *att* sites located on the *E. coli* chromosome. (**A**) Integrative and excisive recombination promoted by 'Int' and 'Int + Xis'. In the presence of Int, recombination between *att*B and *att*P sites generates *att*L and *att*R sites. In the absence of Xis, the inverted configuration is blocked and restoration of the initial state will be possible only in the presence of Int and Xis. (**B**) *att*P and *att*B cassettes allowing phenotypic detection of recombined fragments. A 27-bp fragment corresponding to λ *att*B has been inserted in-frame in the *lacZ* coding region. Integrative recombination disrupts *lacZ* integrity. A reciprocal transaction between *att*L and *att*R cassettes restores *lacZ* integrity. (**C**) Recombination between directly repeated *att* sites. Recombination between directly repeated *att*L and *att*R sites located on the same chromosome results in a deletion of the intervening fragment A (1, excisive deletion). Recombination between *att*L and *att*R sites located on different chromatids provokes duplication of the intervening fragment A on one of the two chromatids and deletion of the same fragment on the other chromatid (2). Identity of the *att* site between the duplicated fragments (*att*B or *att*P, *att*B in the example shown) varies with the position of *att*L relative to that of *att*R. (**D**) Recombination between inverted *att*L and *att*R sites located on the same chromosome results in inversion of the intervening fragment A (1, excisive inversion). Recombination between *att*L and *att*R sites located on different chromatids provokes the formation of a palindromic chromosome dimer presumably lethal (2) (Nash, 1996).

excisionase Xis (Figure 1A). In the absence of Xis, the configuration *att*L–*att*R is blocked and restoration of the initial state *att*P–*att*B is possible only in the presence of Int and Xis. In the presence of Xis, Int-mediated recombination between *att*P and *att*B is inhibited insuring an efficient *att*L–*att*R reaction. Therefore, the sense of recombination is controlled; inverted fragments are stable and consequently easy to score.

This study required the development of two types of tools to generate and quantify DNA recombination. First, *att* cassettes were designed to detect recombination between *att* sites: an in-frame fusion of *att*B in *lacZ* that retained lacZ function was engineered such that recombination with *att*P leads to *lacZ* disruption, and consequently to the formation of cells devoid of β-galactosidase activity. The opposite reaction between *att*L and *att*R restores *lacZ* integrity (Figure 1B). Second, to control recombination, the *int* gene or *xis* and *int* genes were cloned downstream of promoter λ P_R, which is under control of the thermosensitive λ *c*I857 repressor (see Materials and methods). Conditions that provide the optimal amount of recombinase and allow the segregation of recombined chromosomes were experimentally determined (Figure 2 and Materials and methods). Temperature and time of induction for recombinase expression were determined such that, for any combination of *att* sites, the percentage of recombinants never reached 100% (Figure 2A and Materials and methods). A period of 2 h following the induction of recombinase was required to segregate recombinants (Figure 2B).

E. coli cells growing exponentially contain several genomes; the detected recombination events might correspond to recombination reactions within a chromosome, between sister chromatids or between duplicated chromosomes. Directly repeated *att* sites allow one to detect 'intermolecular' events (Figure 1C), whereas inversely oriented *att* sites generate viable recombinants only upon intrachromosome events (Figure 1D).

A total of 14 sets of strains were generated to analyse recombination events (Table I and Supplementary Tables I and II). Each set carried an *att* site at a fixed position (*att*R_{17} indicating for example a fixed *att*R at 17 min on the chromosome

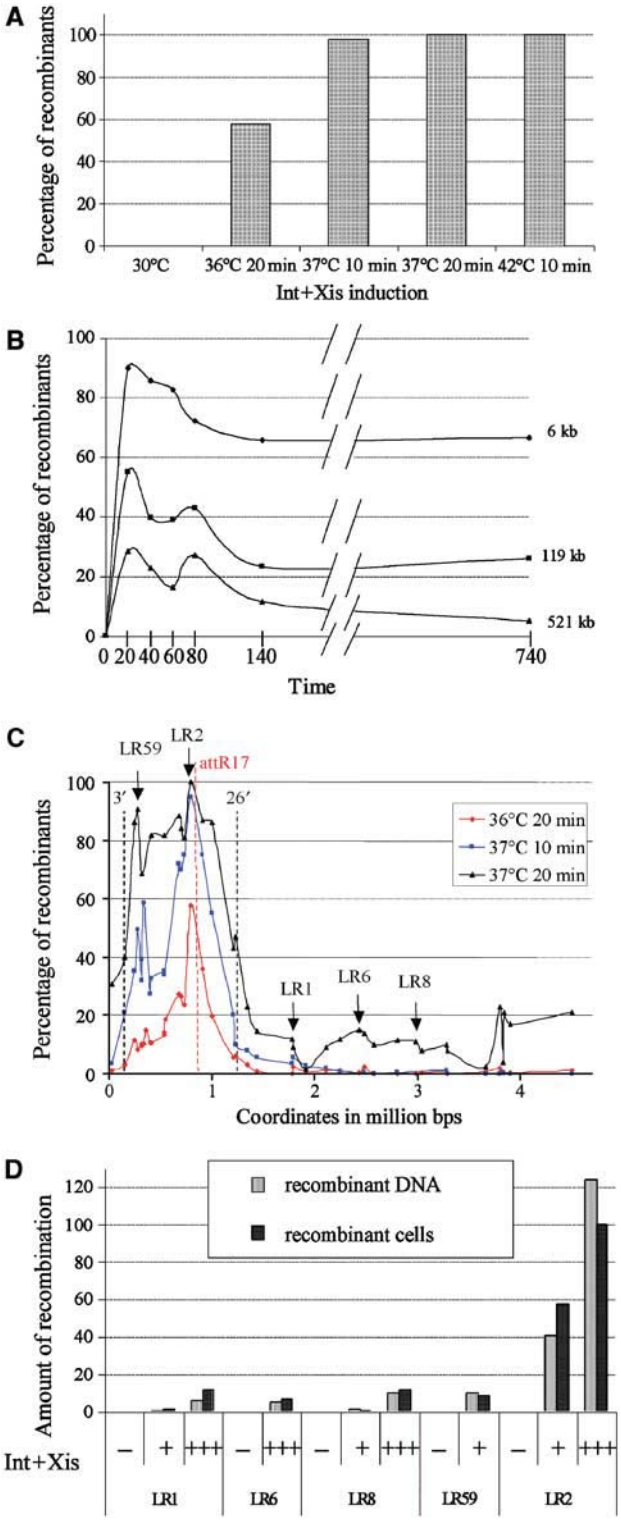

Figure 2 Long-distance DNA interactions revealed by excisive recombination. (**A**) Excisive recombination of 6-kb fragment (strain LR2) promoted by different amounts of recombinase. Int + Xis induction was performed for different times at different temperatures. The *x*-axis indicates conditions providing the amount of Int + Xis synthesized. (**B**) Kinetics of excisive inversions of 6 kb (LR2, indicated by diamonds), 119 kb (LR19, indicated by squares) and 521 kb (LR59, represented by triangles) fragments. Culture samples were plated 20, 40, 60, 80, 140 and 740 min after the beginning of the Int + Xis induction (20 min at 36°C as deduced from (A)). The high level of recombinants in the early time points resulted from the high efficiency of excisive recombination and the incomplete segregation of the recombined chromosomes. The segregation of recombinant chromosomes was achieved after 120 min since the number of recombinant clones became stable after that time and the colonies became uniform. (**C**) Long-range DNA interactions are restricted to subregions of the chromosome. Percentage of recombinants obtained between *att*R_{17} and variously inserted *att*L sites with three different Int + Xis amounts (red line, 20 min of induction at 36°C; blue line, 10 min of induction at 37°C, black line, 20 min of induction at 37°C). The *x*-axis indicates the nt coordinates of the chromosome and *att*R_{17} is indicated by a vertical dashed red line. The 3′ and 26′ regions are indicated. Positions of *att*L sites from strains used in (D) are indicated. (**D**) The percentage of recombinants is similar to the amount of recombination detected by qPCR: the percentage of recombinants (dark grey) is reported beside the percentage of recombinant DNA (light grey). The amount of recombination between *att*L and *att*R was estimated by qPCR in strains LR1, LR6, LR8, LR59 and LR2 (indicated in (C)) with different amounts of Int + Xis (20 min induction at 36°C (+), 20 min induction at 37°C (+ + +)). The value greater than 100% for the amount of recombined *lacZ* DNA in the sample LR2 in (+ + +) condition of recombinase was obtained because it is calculated upon normalization with the control *aadA*.

Table I Percentage of duplications obtained by excisive recombination

Strain name	*att* partner coordinates	Genetic position	Distance *att*L–*att*R (kb)	Recombination (%)
Set FBG146, attR$_{17}$ clockwise at 806549 (17′36)				
LR51	1096182	23′60	289	<0.7
LR21	1334360	28′74	527	0.5
LR66	1368905	29′49	562	0.1
Set FBG146^{off}, attR$_{17}^{off}$ counterclockwise at 806549 (17′36)				
LR177 off	735123	15′84	75	<0.3
LR19 off	682256	14′68	124	<0.9
LR48 off	541911	11′66	264	0.9
Set FBG150-attL$_{29}$, attL clockwise at 1379816 (29′72)				
LC3-R43	1292650	27′85	87.1	3.3
LC3-R50	1226269	26′43	153.4	<0.7
Set FBG150-attL$_{66}$, attL clockwise at 3075618 (66′28)				
LC2-R82	3064833	66′05	10.7	0.5
Set FBG150-attL$_{83}$, attL clockwise at 3857786 (83′14)				
LC5-R33	3835044	82′65	22.7	1.4
LC5-R30	3787239	81′62	70.5	1.2

map) and partner *att* sites inserted at various loci (up to 41 according to the set).

Recombination between duplicated chromatids is a rare occurrence

To determine how frequently *att* sites located on duplicated chromosomes collide, strains that can support *lacZ* reconstitution by intermolecular recombination between *att* sites separated by varying distances (from 10 to 562 kb) were subjected to the recombination test (Figure 1). We used five strain sets, each of them with a defined *att* site. Intermolecular recombination tests were performed in four different regions of the chromosome, with strains containing as fixed *att* site *att*R$_{17}$, *att*R$_{17}^{off}$ (orientation of *att*R$_{17}$ has been inversed), *att*L$_{29}$, *att*L$_{66}$ and *att*L$_{83}$. No recombinants were detected in any strain at a ratio above 3.3% (Table I). The low occurrence of duplications for these intervals did not result from the impossibility of these particular sites to recombine, since deletions provoked by intramolecular recombination events involving these *att* sites were detected (see Supplementary data). The low recombination rate obtained with *att* sites present on duplicated molecules indicates that interactions between sister chromatids or duplicated chromosomes are not frequent.

Long-distance DNA interactions are restricted to within subregions of the chromosome

The analysis of long-distance DNA interactions was performed by determining the amount of excisive recombination in 11 strain sets carrying a fixed *att* site and partner's *att* sites inserted at various positions (Supplementary Table I). To determine the limits of the competent zones for recombination and select the criteria for recognizing putative domains, the amount of excisive recombination was first recorded for the set of 41 strains carrying *att*R$_{17}$ and *att*L inserted at various positions (Supplementary Table I) with different amounts of recombinase. The percentage of recombinants was reported as a function of the position of the variable *att*L site (Figure 2C). The comparison of the profiles obtained with the three amounts of recombinase showed clearly that *att*L sites located in the interval 3′–26′ interacted preferentially with *att*R$_{17}$. In the presence of a nonsaturating amount of recombinase (20 min induction at 36°C), only *att*L sites located in the region between 3′ and 26′ of the chromosome could support inversion with *att*R$_{17}$ at a rate above 3%. The recombination rate decreased with the distance between *att*L and *att*R sites; however, this decrease was not symmetrical. In the clockwise (CW) direction, the most distal *att*L sites that gave rise to inversion at high frequency are found at 420 kb, whereas in the counterclockwise (CCW) direction, sites located up to 646 kb interacted with *att*R$_{17}$ (Table II and Supplementary Table I). The number of recombinants varied from 57% when the recombination interval was 6-kb long to about 3% with longer intervals within the competent region, while the frequency varied from less than 0.1 to 3% for sites located in other regions of the chromosome. When a nearly saturating amount of recombinase (10 min induction at 37°C) was provided, the same chromosomal region (3′–26′) remained competent for inversion from *att*R$_{17}$ (Figure 2C). When a saturating amount of recombinase (20 min induction at 37°C) was provided, higher recombination frequencies were observed in strains carrying *att*L sites, both within the 3′–26′ interval and outside this interval, with percentages between 10 and 20% for many of the latter strains (Figure 2C).

The low percentage of recombinants in strains carrying *att*L outside the interval 3′–26′ might reveal a low probability of collisions between *att*R$_{17}$ and these sites, or might originate from a biased recovery due to poor viability of strains that underwent a large inversion event. If the low percentage of recombinants resulted from a low collision frequency between partner *att* sites, increased amounts of recombinase should allow the detection of sporadic collisions between

Table II Extent of competent zones for inversion

Reference *att* SITE	CCW[a] direction (kb)	CCW[b] limit	CW[a] direction (kb)	CW[b] limit	Extent (Mb)
*att*L$_7$	1183	70′–81′	675	26′–21′	1.75
*att*R$_{17}$/*att*R$_{17}^{off}$	646	0′–3′	420	28′–26′	1.08
*att*R$_{22}$	895	0′–3′	171	28′–26′	1.06
*att*L$_{29}$	150	26′–26.5′	823	49′–47′	0.97
*att*R$_{53}$	255	41′–47′	911	74′–72′	1.16
*att*L$_{70}$	867	44′–51′	1273	1′–97′	2.13
*att*L$_{87}$	961	56′–62′	1195	13′–12′	2.15

[a]Indicates the maximal distance between partner *att* sites that give rise to a recombination rate greater than 3% with a nonsaturating amount of recombinase (induction of 20 min at 36°C).
[b]Indicates the genetic position of the predicted limit of the competent zone for inversions from the considered *att* site. The first value indicates the position of the most proximal site recombining at a rate below 3%, whereas the second value corresponds to the most distal site recombining at a rate above 3% (see text).

attR_{17} and *att*L sites located outside the 3′–26′ interval. On the other hand, effects on viability caused by a large inversion should affect the ratio of blue to white colonies compared to that of recombined DNA. To discriminate between these two possibilities, a real-time quantitative PCR (qPCR) assay was carried out to compare the amount of recombined DNA and the percentage of recombinants. The qPCR assay was used to estimate the proportion of recombined chromosomes obtained with two amounts of recombinase, for five strains having different recombination frequencies (Figure 2D). For strains with *att*L in the 3′–26′ interval (LR2 and LR59 in Figure 2D), recombined DNA was readily detected in the presence of nonsaturating amounts of recombinase (indicated by (+)), and the percentage of recombined chromosomes by qPCR was similar to that determined by the genetic test. For strains with *att*L outside the 3′–26′ interval (LR1, LR6 and LR8 in Figure 2D), the amount of recombined DNA was low with nonsaturating amounts of recombinase, but increased in saturating conditions of recombinase (indicated by (+++)); with both amounts of recombinase, the genetic and qPCR determinations gave concordant results (Figure 2D). The qPCR assay indicates that the determination of recombinants was a satisfactory reflection of the probability of collision between *att* sites and that the low percentage of recombinants with strains carrying *att*L outside the interval 3′–26′ originated from a low probability of collisions of these sites with *att*R_{17}.

The results obtained from *att*R_{17} with three amounts of recombinase allow one to define limits of competent zones for inversion (approximately between 3′ and 26′; Figure 2C): in nonsaturating conditions of recombinase, the limits correspond to the intervals located between the most distal site recombining above 3% (LR35 and LR161; Supplementary Table I) and the most proximal site recombining below 3% (LR11 and LR21 (set *att*R_{17}^{off}); Supplementary Table I). In subsequent analyses, the 3% cutoff level of recombination will be applied to define the limits of the competent zones for inversion. In these conditions of nonsaturating recombinase, the percentage of recombinants was reproducible from experiment to experiment (Supplementary Figure 1). In agreement with the prediction that these recombination events resulted from intrachromosomal events, we observed the same pattern of recombination in cells grown in minimal medium (data not shown), which contain less chromosome units per cell (Akerlund *et al*, 1995).

Chromosomal organizational features limit long-range DNA interactions

The extent of the region colliding with *att*R_{17} does not appear to be symmetrical with regard to *att*R_{17}. To uncover the parameters that determine the range of distant DNA collisions, the limits of the competent zone for inversion from another fixed position in this region, that is, *att*R_{22}, were identified. The inversion percentages of a series of *att* intervals were measured and reported as a function of the position of the variable *att* site with two different amounts of recombinase (Figure 3A). The results indicated that only *att*L sites located in the region between 6′ and 26′ of the chromosome could support inversion with *att*R_{22} in the presence of a nonsaturating amount of recombinase (20 min induction at 36°C). In the CW direction, the most distal *att*L sites that gave rise to inversion at high frequency are found at 171 kb, whereas in the CCW direction, a site located at 738 kb still collided with *att*R_{22}. As seen from *att*R_{17}, increasing the amount of recombinase (10 min induction at 37°C) revealed that the 3′–26′ region was found competent for inversion from *att*R_{22} (Figure 3A): in the CCW direction, sites as distant as 895 kb collide with *att*R_{22} (LRHK35 in Supplementary Table I), whereas the limit of the competent zone did not change in the CW direction. These results indicate that sites located in the 17′–22′ region interact with sites located up to 3′ in the CCW direction but do not collide with sites located beyond 26′ in the CW direction.

To confirm the restrictions to DNA interactions from the 17′–22′ region beyond 26′, the amount of excisive recombination was recorded from a site located beyond 26′, that is, *att*L_{29}. We selected site *att*L_{29}, inserted between Ter sites and located outside the non-divisible zones (NDZs) and the *Dif* activity zone, because this location avoids deleterious effects associated with inversions involving these loci (for review, see Capiaux *et al*, 2001). The inversion frequencies for strains carrying as fixed site *att*L_{29} and *att*R inserted at various loci were determined and reported as a function of the position of the variable *att*R site (Figure 3A). All *att*R insertion sites that gave rise to efficient recombination were located in one subregion of the chromosome, between 26′ and 47′ (Figure 3A and Supplementary Table I). Therefore, in the CCW direction, the most distal site that gave rise to inversion at a significant rate was found at 150 kb, whereas in the CW direction, a site up to 823 kb away still recombined above 3%. This result confirms that the recombination frequency was determined not just by the size of the interval between *att* sites. Rather, the probability of collision between sites straddling 26′ is low.

Genetic characterization of a macrodomain

Interestingly, the limits of the competent region from *att*R_{17} or *att*R_{22} (3′ and 26′; Figure 3A) coincide with the limits of the Ori and Ter macrodomains defined by Niki *et al* (2000). Similarly, the limits of the competent region defined from *att*L_{29} (26′ and 47′; Figure 3A) coincide with the limits of the Ter macrodomain (Niki *et al*, 2000). To further analyse the 3′–26′ region, we determined the limits of the competent zone for inversions from another fixed position in this region, that is, *att*L_7. The inversion percentages of a series of *att* intervals were measured and reported as a function of the position of the variable *att* site (Figure 4A). The pattern obtained indicated that the zone competent for inversion from *att*L_7 was wider than that obtained from *att*R_{17} or *att*R_{22} (1.75 versus 1.08 Mb; Table II). With *att*L_7, whereas the limit in the CW direction was unchanged, around 26′, the limit in the CCW direction is now located at 1183 kb, close to 81′ (Figure 4A), that is, the other limit of the Ori macrodomain. Remarkably, the percentage of recombinants is as great for a site 1183 kb away (10.1%) as for sites 599 kb (10.9%) or 668 kb away (12.8%, LC4R30 versus LC4R32 or LC4R45 in Supplementary Table I), indicating that the large size of the competent inversion zone from *att*L_7 does not result from an increase in reactivity of this site but rather from the possibility to collide with more distant DNA sites.

These results suggested that the interval between 3′ and 26′ contains two different zones, one exemplified by *att*R_{17} and *att*R_{22} from which collisions with partner sites are restricted to the 3′–26′ part and one exemplified by *att*L_7

from which interactions are possible with sites included both in the Ori macrodomain and in the 3′–26′ region. To confirm this hypothesis and map the limits of these two regions, a number of *att*L–*att*R combinations located in the 94′–14′ were analysed (Figure 4C); collisions between *att*L inserted at various locations (*att*L_8, *att*L_{12} and *att*L_{14}) were recorded with different *att*R sites (*att*R_{94}, *att*R_{97} and *att*R_6). Whereas inversions between *att*L_8 or *att*L_{12} were readily detected with *att*R_6, *att*R_{97} or *att*R_{94} (Figure 4C), *att*L_{14} interacted only with *att*R_6 and not with *att*R_{94} or *att*R_{97} (located in the Ori macrodomain; Supplementary Table I). These results confirmed the existence of two regions in the 3′–26′ interval (Figure 4D): DNA sites located in the 3′–12′ interval can collide with sites present in the Ori macrodomain and with sites in the 3′–26′ interval. In contrast, sites in the 14′–26′ interval can interact only with sites present in the 3′–26′ interval. Altogether, these results indicated that collisions between distant DNA sites are restricted to different subregions of the chromosome, which we call hereafter as macrodomains. From the interval 14′–26′, defined hereafter as Right macrodomain, the probability to collide with sites outside the 3′–26′ interval is low. From the 3′–12′ interval, collisions with sites present in both Ori and Right macrodomains are high, suggesting the existence of a less-structured region that can interact with both flanking macrodomains. The *E. coli* chromosome thus has a defined conformation in the cell.

Four macrodomains and two less-structured regions in the E. coli chromosome

To further probe the conformation of the *E. coli* chromosome and define other macrodomains, we analysed the inversion patterns from *att* sites inserted at three different positions in other regions of the chromosome (53′, 70′ and 87′ in Figure 5A). As described above for patterns from *att*L_7, *att*R_{17}, *att*R_{22} or *att*L_{29}, we observed that long-distance interactions were restricted to subregions of the chromosome from each of the reference *att* sites. The sizes of the competent zones for inversion varied from 0.92 to 2.15 Mb (Table II) and the different patterns observed supported the existence of four macrodomains and two less-structured regions in the *E. coli* chromosome.

The pattern of inversions obtained with the set of strains carrying *att*L_{70} was reminiscent of that obtained with the set of strains containing *att*L_7: DNA collisions occurred between *att*L_{70} and sites located between 51′ and 97′, that is, in both the Ori macrodomain and the interval between Ter and Ori macrodomains (Figure 5A). No interactions were detected with sites present in the 1′–44′ interval, indicating that the

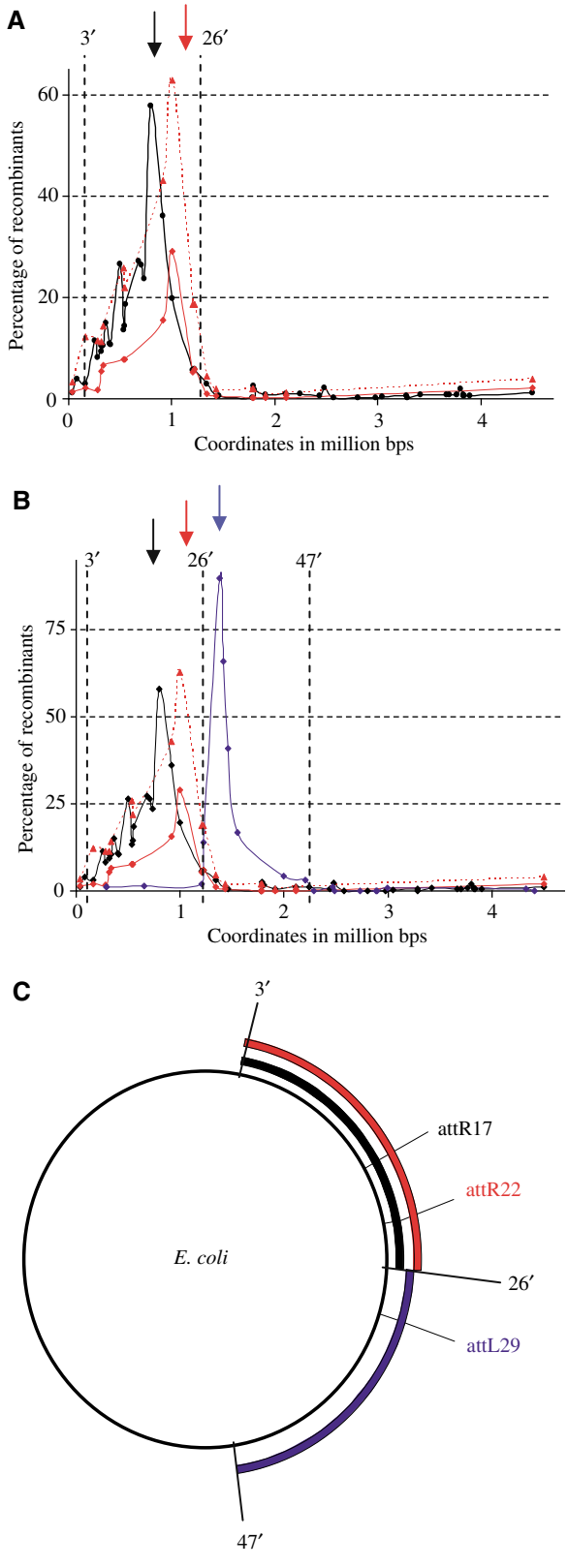

Figure 3 Chromosomal organization features limit long-range DNA interactions. (**A**) Percentage of recombinants obtained by excisive inversion in two sets of strains carrying one fixed *att* site (*att*R_{17}: black; *att*R_{22}: red) and variously inserted partner *att* sites with two different Int + Xis amounts (continuous line, 20 min induction at 36°C; dashed line, 10 min of induction at 37°C). The *x*-axis indicates the nt coordinates of the chromosome. The arrows above the profile indicate the position of the fixed *att* site (*att*R_{17}: black; *att*R_{22}: red). The 3′ and 26′ regions are indicated. (**B**) Percentage of recombinants obtained by excisive inversion in three sets of strains carrying one fixed *att* site (*att*R_{17}: black; *att*R_{22}: red; *att*L_{29}: blue) and variously inserted partner *att* sites with two different Int + Xis amounts (continuous line, 20 min of induction at 36°C; dashed line, 10 min of induction at 37°C). The arrows above the profile indicate the position of the fixed *att* site (*att*R_{17}: black; *att*R_{22}: red; *att*L_{29}: blue). The 3′, 26′ and 47′ regions are indicated. (**C**) Graphical representation of the extent of regions competent for recombination deduced from the inversion profiles obtained in (A, B). The circle represents the genetic map of the chromosome. The coloured bars indicate the competent regions from each fixed *att* site, the position of which is indicated.

CW limit of the zone competent for inversion from *att*L_{70} coincides with the CW limit of the Ori macrodomain whereas the CCW limit is close to 47′, the CW limit of the Ter macrodomain defined above (Table II). These results indicated that *att*L_{70} is located in a region that is analogous to the 3′–12′ less-structured region and that can interact with both the Ori macrodomain and the interval between Ori and Ter macrodomains (Figure 5A and see below).

The presence and the limits of two less-structured regions flanking the Ori macrodomain were confirmed by the inversion profile obtained with the set of strains containing as fixed *att* site *att*L_{87}. From *att*L_{87} that is located near the middle of the Ori macrodomain, interactions were found with *att*R sites located in the interval 62′–12′ (Figure 5A), that is, in the Ori macrodomain (from 81′ to 1′) and in the two less-structured flanking regions (from 62′ to 81′ and from 3′ to 12′, respectively) as predicted from Figure 4, profile *att*L_7 and profile *att*L_{70}. These results also indirectly indicated the existence of a Left macrodomain: DNA sites located in the 47′–62′ interval interact with *att*L_{70} but not with *att*L_{87}. The existence of the Left macrodomain was confirmed by the inversion profile obtained with a set of strains containing as fixed *att* site *att*R_{53}. As predicted, the CCW limit was found between 41′ and 47′, that is, coincides with the CW limit of the Ter macrodomain. In the CW direction, *att*R_{53} collides with sites as distant as 911 kb, setting the CW limit close to 75′. As observed with *att*R_{22} (Figure 3), an increase of the amount of recombinase allowed interaction with sites located up to 76′ but not with sites present beyond 80′, that is, in the Ori macrodomain (data not shown). Altogether, these results indicate that the *E. coli* chromosome contains two less-structured regions flanking the Ori macrodomain and two structured regions, the Left and Right macrodomains, flanking the Ter macrodomain (Figure 5B).

Integrative inversions reveal the same long-distance DNA interactions

Biochemical analyses have revealed that integrative (*att*B–*att*P) and excisive (*att*L–*att*R) recombinations differ in several ways. First, integrative recombination is dependent on the level of *att*P supercoiling, whereas excisive recombination does not require supercoiled *att* sites (Azaro and Landy, 2002). Second, topological analyses have revealed that the two reactions promote the formation of products with different topologies (Crisona *et al*, 1999). Third, we have found in this assay that excisive recombination is far more efficient than integrative recombination (see Materials and methods). To determine whether long-range DNA collisions revealed by integrative recombination were similar to those uncovered by

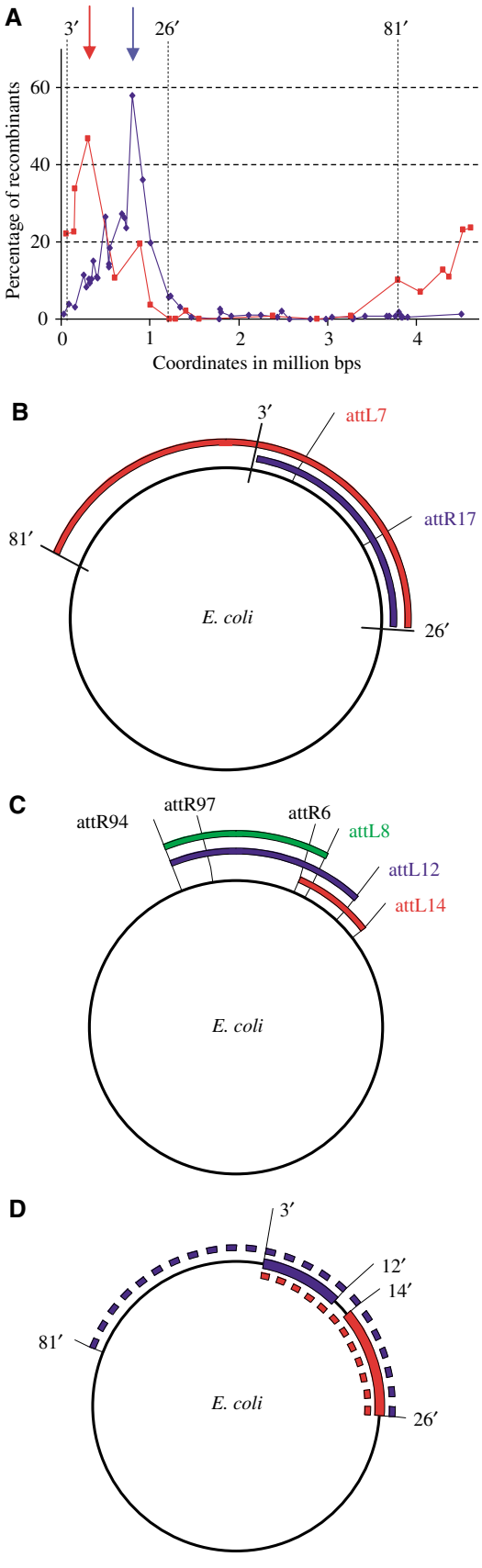

Figure 4 Genetic characterization of a macrodomain. (**A**) Percentage of recombinants obtained by excisive inversion in two sets of strains carrying one fixed *att* site (*att*R_{17}: blue; *att*L_7: red) and variously inserted partner *att* sites. The *x*-axis indicates the nt coordinates of the chromosome. The arrows above the profile indicate the position of the fixed *att* site (*att*L_7: red; *att*R_{17}: blue). The 3′, 26′ and 81′ regions are indicated. (**B**) Graphical representation of the extent of regions competent for recombination deduced from the inversion profiles obtained in (A). (**C**) Graphical representation of long-range interactions between various *att*R and *att*L sites. The extent of the arc indicates the range of interactions. (**D**) Graphical representation of the Right macrodomain and the less-structured region. Coloured bars represent the different regions (red: Right macrodomain; blue: less-structured region). Coloured interrupted bars schematize the extent of inversion competent zones from sites located in the respective coloured intervals.

excisive recombination, the pattern of interactions deduced from integrative recombination frequencies was performed (data not shown). The amount of integrative inversion was recorded for the set of 33 strains carrying *att*B_{17} inserted in-frame in *lacZ* and *att*P inserted at various loci. The inversion frequencies for each of these clones were determined (Supplementary Table II); *att*P sites able to support inversion above 3% were found in the 3′–26′ interval. Because the two types of reactions rely on different processes to perform synapsis of *att* sites, the findings that zones competent for inversion from att_{17} were similar for the two types of reactions indicated that the assays reflected the probability of collisions between distant DNA sites.

Discussion

Organization of the chromosome into macrodomains

We have shown that the *E. coli* chromosome appears to be subdivided in large regions referred to as macrodomains in which DNA interactions occurred preferentially. DNA interactions between these different macrodomains are highly restricted. The principle of the method was to select many pairs of inversely oriented *att* sites that can give rise to inversions of the intervening fragment, to provide a limiting amount of recombinase that will not saturate the recombination reaction between any combination of sites and to measure the extent of recombination. These three steps have potential limitations for this study and are discussed below.

By using a system of programmed genetic DNA transactions, we were able to characterize 211 combinations of *att* sites that support recombination. This method is different from other approaches that have been used previously (Rebollo *et al*, 1988; Segall *et al*, 1988). In these systems, viable, detrimental or forbidden inversions were revealed but there was no direct measure of spatial chromosome organization. Our experimental design eliminated combinations of sites that gave rise to nonviable or forbidden inversions since we selected only clones able to support recombination. Among clones competent for inversions, the measure of recombination rates allowed the identification of macrodomains and does not preclude the existence of nonviable or forbidden inversions in macrodomains.

The second critical feature of the method was the amount of recombinase that was provided; in pilot tests, we set up conditions that provide the optimal amount of recombinase taking into account that an excessive amount of recombinase, saturating some combinations of sites, will diminish the differential of interactions (Figure 2).

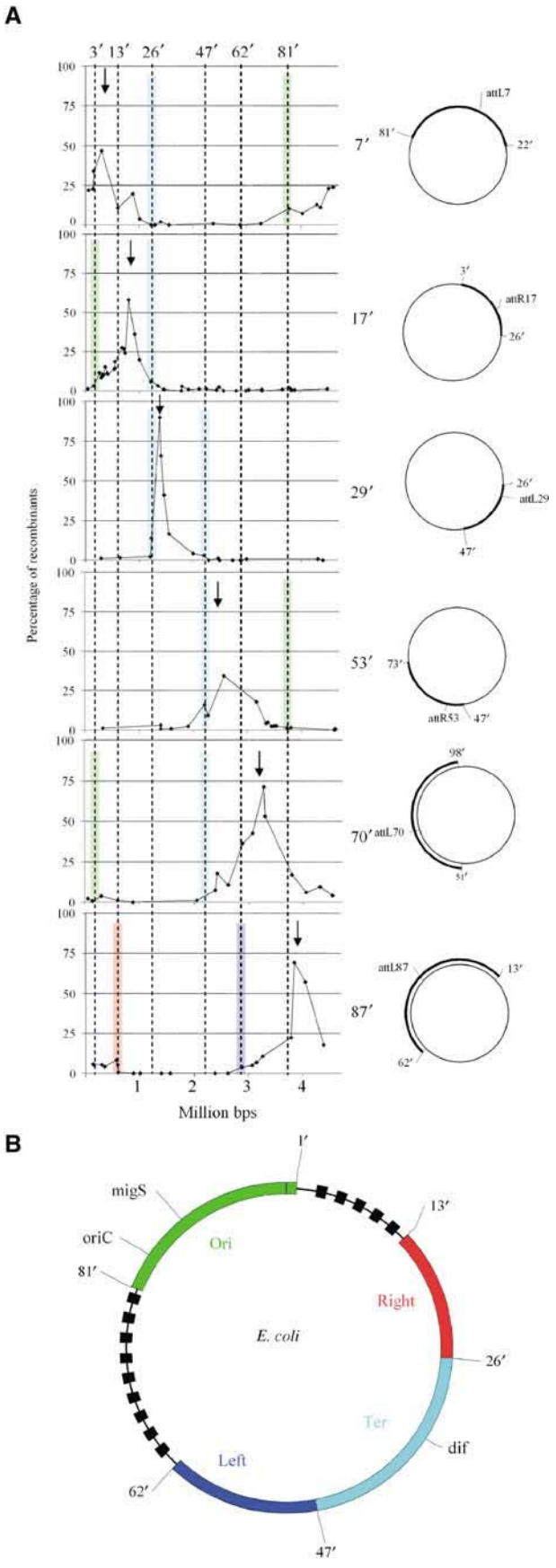

Figure 5 Genetic characterization of macrodomains. (**A**) Percentage of recombinants obtained by excisive inversion in different sets of strains carrying one fixed *att* site and variously inserted partner *att* sites. The *x*-axis indicates the nt coordinates of the chromosome. The position of the fixed *att* site is indicated on the right of the panels and by the arrow above the profile. Dashed vertical lines indicate the delimitation of macrodomains and other regions indicated above the profile *att*L_7 and shown in (B). Beside each profile is indicated a graphical representation of the profile on the genetic map. (**B**) Graphical representation of *E. coli* macrodomains and less-structured regions. The circle represents the genetic map of the chromosome. Coloured bars represent the different macrodomains and interrupted black bars schematize two less-structured regions. Replication origin *oriC*, *migS* and *dif* sites are indicated.

Finally, by using a qPCR assay, we unambiguously showed that the percentage of recombinant clones reflected satisfactorily the fraction of DNA that recombined, indicating that no bias was introduced in the assay and that the measure of recombinant clones was appropriate to disclose the conformation of the bacterial chromosome (Figure 2).

For all profiles, interactions were restricted to subregions of the chromosome that included the reference *att* site and regions contiguous to this reference site. In many cases, we observed a decrease in the recombination frequency with distance. In nonsaturating conditions of recombinase, we did not detect any preferential interactions with a noncontiguous region or even with a region diametrically opposed relative to the *oriC–dif* axis or to the Ori–Ter macrodomain axis. At first sight, these results appear consistent with a model for *in vivo* synapis assembly involving tracking from one att site rather than relying on random collision of *att* sites. However, although this model is attractive, it can be ruled out for several reasons. First, in a tracking model, the level of recombination should decrease with distance, but this is not always the case. For example, the percentage of recombinants is similar for sites 599, 668 or 1183 kb away from *att*L_7. Second, we have observed that in cells containing specific rearranged chromosomes, preferential interactions were detected with noncontiguous regions (Valens *et al*, in preparation). Instead of resulting from a tracking mechanism, the observed small decrease in recombination with distance, within macrodomains, might originate from the condensed ring organization of the chromosome (see below) because increasing the distance between the *att* sites will diminish the probability of collision of these sites in space.

Limited chromatid interactions

With the use of directly repeated sites, we could monitor duplication that occurs necessarily by intermolecular recombination. These results show that ability to support intermolecular recombination is rare in the chromosome. Fluorescence approaches gave contradictory results about the extent of cohesion between the two *oriC*-proximal halves of the *E. coli* chromosome after replication: Sunako *et al* (2001) observed a long period of cohesion, whereas in two different reports cohesion was estimated to be very short (Li *et al*, 2002; Lau *et al*, 2003). Our results of interchromatid recombination support the extrusion capture model (Lemon and Grossman, 2001).

Macrodomains and spatial organization of the chromosome

Our data clearly demonstrated that, in *E. coli*, sites do not interact equally with the different parts of the chromosome and the great number of *att* pair's combinations analysed allowed us to map macrodomains and less-constrained regions. Our results must be compared with those obtained using FISH by Niki *et al* (2000). We were able to predict four macrodomains and two less-structured regions (Figure 5B), whereas FISH disclosed only two macrodomains. Ori and Ter macrodomains defined here remarkably coincide with Ori and Ter FISH macrodomains respectively, indicating that the structuring mechanism revealed by the genetic approach is stable enough to resist cell biology techniques.

The observations reported here indicate that the left and right intervals between Ori and Ter macrodomains are not linker DNA, but that a part of these exists also as organized Left and Right macrodomains, respectively. The absence of communications between an *att* site inserted at 17′ and sites diametrically opposed relative to an axis *oriC–dif* suggests a strict spatial localization of the Right and Left macrodomains. From *att*R_{17}, collision occurs with sites distant of 650 kb, but interactions with the opposite replichore are very limited, although these regions were seen in FISH experiments along the cell's long axis (Niki *et al*, 2000). It is also interesting to note that although the region present between the Right and Ori macrodomains appeared to be less structured because it can interact with both flanking macrodomains, it does not interact with other parts of the chromosome, indicating limited flexibility of this region.

The biased interactions detected in this study highlight two different phenomena: condensation of the DNA molecule and sequestration of macrodomains. It is remarkable that within a macrodomain, the condensation of the DNA molecule allows the interaction of sites more than 500 kb away. On the other

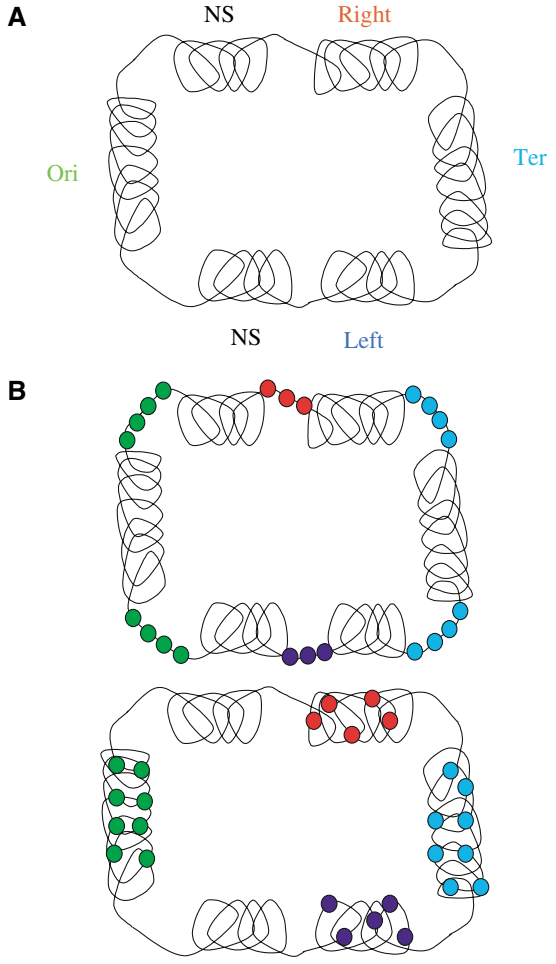

Figure 6 A model for chromosome organization in *E. coli*. (**A**) The chromosome is organized as a ring composed of four macrodomains (Ori, Ter, Right and Left) and two less-structured regions (NS) with flexibility limited to the flanking macrodomains. (**B**) Two models for the spatial sequestration of macrodomains. On the top, organizing factors bind to DNA separating different regions and defining the different macrodomains. On the bottom, binding of a number of determinants by unidentified factors concentrates DNA regions containing these sites and defines macrodomains. The second model is favoured (see text).

hand, macrodomain sequestration inhibits collision of sites situated in different macrodomains. Altogether, these results indicate that the chromosome is organized as a ring composed of four macrodomains and two less-structured regions with flexibility limited to the flanking macrodomains (Figure 6A).

Two major processes could account for this chromosome structuring (Figure 6). First, macrodomains may be separated by DNA structures that disfavour interactions (Figure 6B, top). Alternatively, it is possible that the different macrodomains are insulated in different parts of the cell and that the specific localization maintains DNA separation; sequestration of large regions would imply the presence of determinants present in the macrodomain (Figure 6B, bottom). Three different arguments indicate that the second scenario is more likely to apply to the *E. coli* chromosome (Figure 6B, bottom). First, since synapsis of *att* sites occurs by random collision, it is hard to conceive from the first hypothesis how structures on the DNA molecule could inhibit collisions between distant DNA sites. Second, the condensation of a large region harbouring distant DNA binding sites has been described in *B. subtilis* (Lee *et al*, 2003) and it is conceivable that different proteins may help localize different macrodomains of the *E. coli* chromosome. Third, the structuring processes did not impede inversions from *att*L_7 or *att*L_{70} with sites located in both flanking macrodomains implying the absence of fixed barriers. Further experiments will be required to characterize the role and the origin of macrodomains in the cell. A possible reason for this organization is to orchestrate chromosome movements that occurred during the cell cycle. As observed in the B period by Niki *et al* (2000), repositioning of the chromosome seems to be required at specific step(s) in the cell cycle. Orchestrating the movement of a limited number of 'organizing' proteins might be easier than the manipulation of 4.6 Mb of DNA. The characterization of the *E. coli* chromosome organization reveals for the first time the structuring of a complete chromosome into large macrodomains. This study will enable the search for determinants that are responsible for this structuring and may uncover processes that control spatial organization of chromosomes in living cells.

Materials and methods

Strains and plasmids

E. coli K12 strains are all derivatives of MG1655. Standard transformation and transduction procedures used were as described before (Espéli *et al*, 2001). Constructions of strains and plasmids are described in Supplementary data. Plasmids and strains with relevant genotypes are described in Table III.

Selection of strains supporting excisive and integrative recombination

To select for strains that support excisive recombination, 13 sets of strains carrying one fixed *att* site and the partner *att* site inserted at various loci were constructed. For four of the sets carrying one fixed *att* site and variously inserted mobile partner sites (sets of strains carrying *att*R_{17}, *att*L_{29}, *att*R_{53}, *att*L_{82}), a large number of clones were individually transformed with pTSA29-CXI, a plasmid expressing *int* and *xis* under the control of *c*I857 repressor; in the absence of repressor in the cell, introduction of this plasmid by transformation resulted in transient synthesis of Int and Xis and allowed the detection of strains supporting recombination. The location and orientation of mobile *att* sites were then determined by sequence analysis. For the other nine sets, specific combinations of *att* sites were constructed using phage P1 transduction (see Supplementary data). To select for strains that support integrative recombination, several hundred derivatives of FBG140 carrying *att*B_{17} and

Table III Strains and plasmids

Name	Description[a]	Reference or source
Strains		
MG1655 Δlac	Δ*lacIZ Mlu*I	Espéli *et al* (2001)
MC1061	F- *araD139* Δ*(ara-leu)7696 galE15 galK16* Δ*(lac)X74 rpsL hsdR2 mcrA mcrB1*	Lab collection
FBG150	MG1655 Δ*lacIZ* Δ*att*B^{λ}::*aadA*	This work
FBG140	MG1655 Δ*lacIZ* Δ*att*B^{λ}::*aadA*-P_{GBM3}-*lacZ*::*att*B^{λ}-*cat*	This work
FBG146	MG1655 Δ*lacIZ* Δ*att*B^{λ}::*aadA-att*R^{λ}-′*lacZ-cat*	This work
FBG146^{off}	MG1655 Δ*lacIZ* Δ*att*B^{λ}::*aadA-att*R^{λ}-′*lacZ-cat*	This work
FBG147	MG1655 Δ*lacIZ* Δ*att*B^{λ}::*aadA-att*B^{HK022}::*att*R^{λ}-′*lacZ-cat*	This work
FBG150-*att*L_7	FBG150 (*betT-yahA*)::mini-Tn*5-cat*-P_{GBM3}-*lacZ*′-*att*L^{λ}	This work
FBG150-*att*L_{29}	FBG150 (*ycjV-ompG*)::mini-Tn*5-cat*-P_{GBM3}-*lacZ*′-*att*L^{λ}	This work
FBG150-*att*R_{53}	FBG150 *cmtA*::mini-Tn*5-cat*-P_{GBM3}-*lacZ*′-*att*L^{λ}	This work
FBG150-*att*L_{66}	FBG150 *cmtA*::mini-Tn*5-cat*-P_{GBM3}-*lacZ*′-*att*L^{λ}	This work
FBG150-*att*L_{70}	FBG150 *yhaI*::mini-Tn*5-cat*-P_{GBM3}-*lacZ*′-*att*L^{λ}	This work
FBG150-*att*L_{82}	FBG150 *yicO*::mini-Tn*5-cat*-P_{GBM3}-*lacZ*′-*att*L^{λ}	This work
FBG150-*att*L_{83}	FBG150 (*yidK-yidL*)::mini-Tn*5-cat*-P_{GBM3}-*lacZ*′-*att*L^{λ}	This work
FBG150-*att*L_{87}	FBG150 (*ubiB-fadA*)::mini-Tn*10-cat*-P_{GBM3}-*lacZ*′-*att*L^{λ}	This work
Plasmids		
pNKBOR	R6 K replicon carrying mini-Tn*10*, Kn^R	Rossignol *et al* (2001)
pNKBOR-*att*P	pNKBOR carrying *att*P, Kn^R	This work
pNKBOR-*att*L	pNKBOR carrying (P_{GBM3}-*lacZ*′-*att*L), Kn^R	This work
pNKBOR-*att*R	pNKBOR carrying (*att*R-′*lacZ*), Kn^R	This work
pNCBOR	R6 K replicon carrying mini-Tn*10*, Cm^R	This work
pNCBOR-attL	pNCBOR carrying attL, Cm^R	This work
pUT-Tn5-cat-*att*L	pUT-Tn*5-cat* carrying (P_{GBM3}-*lacZ*′-*att*L)	This work
PTSA29-CXI-AK	pTSA29 carrying *c*I857-P_R-*int*$^{\lambda}$	This work
pTSA29-CXI	pTSA29 carrying *c*I857-P_R-(*xis*$^{\lambda}$-*int*$^{\lambda}$)	This work

[a]When the mini-Tn*5* is inserted between two genes, the names of flanking genes are in parentheses. The exact insertion point is given in Table I and in supplementary tables. *lacZ*′-*att*L indicates a fusion of the 5′ part of *lacZ* to *att*L; *att*R-′*lacZ* indicates a fusion of *att*R to the 3′ part of *lacZ*.

variously inserted *att*P sites were transformed with pTSA29-CXI-AK, a plasmid expressing *int* under the control of *c*I857 repressor; incubation at 37°C resulted in synthesis of Int and allowed the detection of strains supporting recombination.

Recombination assays

The recombination test (Figure 2) includes a transient incubation at a higher temperature to inactivate *c*I857 repressor and to promote a pulse of Int (integrative recombination) or Int and Xis (excisive recombination) synthesis, respectively. Because several lines of evidence indicated that reactions of excisive inversion were more efficient than those of integrative inversion, the conditions for Int and Int + Xis induction were different. For excisive inversions and duplications, inductions were performed at 36°C during 20 min (unless otherwise stated), conditions that provide a nonsaturating amount of recombinase and give highly reproducible recombination rates (Supplementary Figure 1). Overnight cultures were diluted 100-fold, grown to an OD_{600} of 0.3 in L medium and submitted to heat shock. A control sample was kept at 30°C. Cultures were kept at 30°C during 120 min before plating cells on L medium containing ampicillin (50 μg/ml) and X-Gal (80 μg/ml). Between 200 and 300 colonies were counted to estimate the recombination rate. For the integrative recombination assay, we noticed that strains carrying different constructions expressing *int* always showed a background level of inversion activity (data not shown). Because of this background level of recombination, clones selected for their ability to support fragment inversion between inversely oriented *att*P and *att*B sites were isolated, streaked twice at 30°C and individual blue clones were inoculated in 10 ml culture of Lennox medium. Because integrative recombination was less efficient (data not shown), the induction was performed at 42°C for 10 min when cultures reach OD_{600} 0.3 and a 2 h incubation time was allowed for the segregation of recombinant chromosomes before plating.

Quantitative PCR

For the quantitative analysis of recombination, fluorescence real-time PCR was performed using dsDNA dye SYBR Green I (Roche Diagnostics). Total DNA was extracted immediately after recombinase induction. Primer pairs were 5′-TTACGCGCCGGAGAAAACCG-3′ and 5′-TCAACCACCGCACGATAGAG-3′ for *lacZ*; 5′-CGACTACCTT GGTGATCTCG-3′ and 5′-CGACATTGATCTGGCTATCTTG-3′ for *aadA*. The amount of recombined *lacZ* DNA detected was normalized with the control *aadA* values.

Identification of the insertion points of att sites

Insertion points of the different minitransposons were determined by direct sequencing of chromosomal DNA using the Big dye terminator Version 3 kit (ABI Prism). Each sequencing reaction contained 10 μg of chromosomal DNA, 40 pmol of primers in a volume of 20 μl and was submitted to 99 PCR cycles (95°C 30 s, 55°C 30 s, 60°C 4 min). Primers used to determine *att* site insertions were 5′-GCAACGAACAGGTCACTATCAGTC-3′ or 5′-TTCCCAGTCAC GACGTTGTAAA-3′ (*att*L), 5′-ATGTTCTAGAGGATCTGTGA-3′ (*att*R) and 5′-TGATGCCTCTAGCACGCGTA-3′ (*att*P). Sequencing reactions were analysed on a 3100 Genetic analyser (Applied Biosystems).

Supplementary data

Supplementary data are available at *The EMBO Journal* Online.

Acknowledgements

We thank Alexandra Gruss, Bénédicte Michel and Linda Sperling for critical reading of the manuscript, Martial Marbouty and Corentin Laulier for performing some inversion experiments, Bob Weisberg for the kind gift of strains and phages, and Laurent Moulin and Olivier Espéli for helpful discussions. This work was supported by the Centre National de la Recherche Scientifique, the Association pour la Recherche sur le Cancer and the Program Microbiologie PRMMIP 295007.

References

Akerlund T, Nordstrom K, Bernander R (1995) Analysis of cell size and DNA content in exponentially growing and stationary-phase batch cultures of *Escherichia coli*. *J Bacteriol* **177:** 6791–6797

Azaro MA, Landy A (2002) Integrase and the Int family. In *Mobile DNA II*, Craig NL, Craigie R, Gellert M, Lambowitz AM (eds) pp 118–148. Washington, DC: ASM Press

Ben-Yehuda S, Rudner DZ, Losick R (2003) RacA, a bacterial protein that anchors chromosomes to the cell poles. *Science* **299:** 532–536

Breier AM, Cozzarelli NR (2004) Linear ordering and dynamic segregation of the bacterial chromosome. *Proc Natl Acad Sci USA* **101:** 9175–9176

Capiaux H, Cornet F, Corre J, Guijo MI, Perals K, Rebollo JE, Louarn JM (2001) Polarization of the *Escherichia coli* chromosome. A view from the terminus. *Biochimie* **83:** 161–170

Case RB, Chang YP, Smith SB, Gore J, Cozzarelli NR, Bustamante C (2004) The bacterial condensin MukBEF compacts DNA into a repetitive, stable structure. *Science* **305:** 222–227

Crisona NJ, Weinberg RL, Peter BJ, Sumners DW, Cozzarelli NR (1999) The topological mechanism of phage lambda integrase. *J Mol Biol* **289:** 747–775

DeBoy RT, Craig NL (1996) Tn7 transposition as a probe of *cis* interactions between widely separated (190 kilobases apart) DNA sites in the *Escherichia coli* chromosome. *J Bacteriol* **178:** 6184–6191

Deng S, Stein RA, Higgins NP (2004) Transcription-induced barriers to supercoil diffusion in the *Salmonella typhimurium* chromosome. *Proc Natl Acad Sci USA* **101:** 3398–3403

Espéli O, Levine C, Hassing H, Marians KJ (2003) Temporal regulation of topoisomerase IV activity in *E. coli*. *Mol Cell* **11:** 189–201

Espéli O, Moulin L, Boccard F (2001) Transcription attenuation associated with bacterial repetitive extragenic BIME elements. *J Mol Biol* **314:** 375–386

Garcia-Russell N, Harmon TG, Le TQ, Amaladas NH, Mathewson RD, Segall AM (2004) Unequal access of chromosomal regions to each other in *Salmonella*: probing chromosome structure with phage lambda integrase-mediated long-range rearrangements. *Mol Microbiol* **52:** 329–344

Higgins NP (1999) DNA supercoiling and its consequences for chromosome structure and function. In *Organization of the Procaryotic Genome*, Charlebois RL (ed) pp 189–202. Washington, DC: ASM Press

Higgins NP, Yang X, Fu Q, Roth JR (1996) Surveying a supercoil domain by using the gamma delta resolution system in *Salmonella typhimurium*. *J Bacteriol* **178:** 2825–2835

Lau IF, Filipe SR, Soballe B, Okstad OA, Barre FX, Sherratt DJ (2003) Spatial and temporal organization of replicating *Escherichia coli* chromosomes. *Mol Microbiol* **49:** 731–743

Lee PS, Lin DC, Moriya S, Grossman AD (2003) Effects of the chromosome partitioning protein Spo0J (ParB) on oriC positioning and replication initiation in *Bacillus subtilis*. *J Bacteriol* **185:** 1326–1337

Lemon KP, Grossman AD (2000) Movement of replicating DNA through a stationary replisome. *Mol Cell* **6:** 1321–1330

Lemon KP, Grossman AD (2001) The extrusion-capture model for chromosome partitioning in bacteria. *Genes Dev* **15:** 2031–2041

Li Y, Sergueev K, Austin S (2002) The segregation of the *Escherichia coli* origin and terminus of replication. *Mol Microbiol* **46:** 985–996

Nash HA (1996) Site specific recombination: integration, excision, resolution, and inversion of defined DNA segments. In *Escherichia coli and Salmonella*, Neidhardt FC (ed) pp 2363–2376. Washington, DC: ASM Press

Niki H, Yamaichi Y, Hiraga S (2000) Dynamic organization of chromosomal DNA in *Escherichia coli*. *Genes Dev* **14:** 212–223

Parada L, Misteli T (2002) Chromosome positioning in the interphase nucleus. *Trends Cell Biol* **12:** 425–432

Postow L, Hardy CD, Arsuaga J, Cozzarelli NR (2004) Topological domain structure of the *Escherichia coli* chromosome. *Genes Dev* **18:** 1766–1779

Rebollo JE, Francois V, Louarn JM (1988) Detection and possible role of two large nondivisible zones on the *Escherichia coli* chromosome. *Proc Natl Acad Sci USA* **85:** 9391–9395

Rossignol M, Basset A, Espeli O, Boccard F (2001) NKBOR, a mini-Tn10-based transposon for random insertion in the chromosome of Gram-negative bacteria and the rapid recovery of sequences flanking the insertion sites in *Escherichia coli*. *Res Microbiol* **152:** 481–485

Segall A, Mahan MJ, Roth JR (1988) Rearrangement of the bacterial chromosome: forbidden inversions. *Science* **241:** 1314–1318

Sherratt DJ (2003) Bacterial chromosome dynamics. *Science* **301:** 780–785

Sunako Y, Onogi T, Hiraga S (2001) Sister chromosome cohesion of *Escherichia coli*. *Mol Microbiol* **42:** 1233–1241

Teleman AA, Graumann PL, Lin DC, Grossman AD, Losick R (1998) Chromosome arrangement within a bacterium. *Curr Biol* **8:** 1102–1109

Viollier PH, Thanbichler M, McGrath PT, West L, Meewan M, McAdams HH, Shapiro L (2004) Rapid and sequential movement of individual chromosomal loci to specific subcellular locations during bacterial DNA replication. *Proc Natl Acad Sci USA* **101:** 9257–9262

Wu LJ, Errington J (1998) Use of asymmetric cell division and spoIIIE mutants to probe chromosome orientation and organization in *Bacillus subtilis*. *Mol Microbiol* **27:** 777–786

Wu LJ, Errington J (2002) A large dispersed chromosomal region required for chromosome segregation in sporulating cells of *Bacillus subtilis*. *EMBO J* **21:** 4001–4011

Yamaichi Y, Niki H (2004) migS, a *cis*-acting site that affects bipolar positioning of oriC on the *Escherichia coli* chromosome. *EMBO J* **23:** 221–233